Molecular Biology of the Cell
Vol. 11, 1845–1858, May 2000

Inositol 1,4,5-Trisphosphate Directs Ca^{2+} Flow between Mitochondria and the Endoplasmic/Sarcoplasmic Reticulum: A Role in Regulating Cardiac Autonomic Ca^{2+} Spiking

Marisa Jaconi,*¶ Claire Bony,* Stephen M. Richards,*# André Terzic,† Serge Arnaudeau,‡ Guy Vassort,* and Michel Pucéat*†§‖

*Institut National de la Santé et de la Recherche Médicale U-390, CHU Arnaud de Villeneuve, Montpellier, 34295 France; §Centre de Recherches de Biochimie Macromoléculaire, Centre National de la Recherche Scientifique UPR 1086, Montpellier, 34293 France; †Division of Cardiovascular Diseases, Department of Medicine and Molecular Pharmacology, Mayo Clinic, Rochester, Minnesota 55905; and ‡Department of Physiology, Centre Médical Universitaire, Genève, Switzerland

Submitted September 27, 1999; Revised January 20, 2000; Accepted February 22, 2000
Monitoring Editor: Guido Guidotti

The signaling role of the Ca^{2+} releaser inositol 1,4,5-trisphosphate (IP_3) has been associated with diverse cell functions. Yet, the physiological significance of IP_3 in tissues that feature a ryanodine-sensitive sarcoplasmic reticulum has remained elusive. IP_3 generated by photolysis of caged IP_3 or by purinergic activation of phospholipase Cγ slowed down or abolished autonomic Ca^{2+} spiking in neonatal rat cardiomyocytes. Microinjection of heparin, blocking dominant-negative fusion protein, or anti-phospholipase Cγ antibody prevented the IP_3-mediated purinergic effect. IP_3 triggered a ryanodine- and caffeine-insensitive Ca^{2+} release restricted to the perinuclear region. In cells loaded with Rhod2 or expressing a mitochondria-targeted cameleon and TMRM to monitor mitochondrial Ca^{2+} and potential, IP_3 induced transient Ca^{2+} loading and depolarization of the organelles. These mitochondrial changes were associated with Ca^{2+} depletion of the sarcoplasmic reticulum and preceded the arrest of cellular Ca^{2+} spiking. Thus, IP_3 acting within a restricted cellular region regulates the dynamic of calcium flow between mitochondria and the endoplasmic/sarcoplasmic reticulum. We have thus uncovered a novel role for IP_3 in excitable cells, the regulation of cardiac autonomic activity.

INTRODUCTION

The signaling role of inositol 1,4,5-trisphosphate (IP_3) via intracellular Ca^{2+} mobilization has been established in many cell types and associated with secretion, neurotransmission, fertilization, cell motility, gene expression, or cell death (Berridge, 1993; Clapham, 1995). In the heart, IP_3 is generated by a plethora of neurohumoral agonists. These include acetylcholine, endothelin, catecholamines, or prostaglandins (Brown *et al.*, 1985; Hilal-Dandan *et al.*, 1992; Adams *et al.*, 1998) that activate a Gq-dependent phospholipase Cβ (PLCβ) or purines or angiotensin II that stimulate a tyrosine kinase–dependent PLCγ (Puceat and Vassort, 1996; Goutsouliak and Rabkin, 1997). Yet, the role of IP_3 in the heart has remained elusive. In cardiac cells, rhythmic changes in membrane potential and associated Ca^{2+}-induced Ca^{2+} release (CICR) from the sarcoplasmic reticulum (SR) are believed responsible for repetitive Ca^{2+} transients. Therefore, it remains an enigma, why would cardiac cells use, in addition to ryanodine receptors (RyR) of the SR, IP_3 receptors (IP_3R) to also regulate Ca^{2+} homeostasis.

Although IP_3 has been implicated in cardiac arrhythmias (Jacobsen *et al.*, 1996), heart failure (Marks, 1997), and graft rejection (Felzen *et al.*, 1997), the significance of IP_3 in cardiac function has remained unresolved, in part, because of confounding effects of abundant RyRs. We here used neonatal rat cardiomyocytes in culture, which feature an immature SR and express a low density of RyRs (Fitzgerald *et al.*, 1994). Such cells exhibit spontaneous, rhythmic action potentials (Jongsma *et al.*, 1983) resulting in repetitive Ca^{2+} oscillations and spontaneous autonomic activity. Development of auto-

‖ Corresponding author. E-mail address: puceat@crbm.cnrs-mop.fr.
¶ Present address: Departement de Geriatrie, Centre Médical Universitaire, Geneva, Switzerland.
# Present address: Division of Biochemistry, University of Tasmania, Hobart, Australia.

maticity in these cells depends primarily on the expression of two ion channels, a hyperpolarization-activated I_f current, with the same range of potential-dependent activation and Cs^+ sensitivity as that found in pacemaker cells of the sinoatrial node, and a transient voltage-dependent Ca^{2+} (I_{CaT}) current (Gomez *et al.*, 1994; Fares *et al.*, 1998). Moreover, the establishment of intercalated disks, gap junctions, and T-tubes (Moses and Kasten, 1979) synchronizes the electrical activity of connected cells. With such cytoarchitectural and electrophysiological properties, neonatal rat cardiomyocytes in culture represent a unique cellular model in which to study the regulation of cardiac autonomic activity.

Here, we show that IP_3 generated by intracellular photorelease of a caged precursor or by purinergic stimulation of cells, and acting on IP_3Rs, triggers a spatially restricted Ca^{2+} release from a ryanodine-insensitive intracellular store. Moreover, IP_3 triggers mitochondrial Ca^{2+} uptake and depolarization associated with SR Ca^{2+} depletion that slows down or arrests autonomic Ca^{2+} spiking. Thus, our results provide the first evidence that in cardiac cells, IP_3-induced Ca^{2+} release from a ryanodine-insensitive pool modulates cardiac autonomic activity via mitochondrial signaling.

MATERIALS AND METHODS

Cell Isolation and Culture

Cardiomyocytes were isolated from 2- to 3-d neonatal rats (Puceat *et al.*, 1994) and kept in culture for 5 d. Purkinje cells were isolated from rabbit hearts as described previously (Scamps and Carmeliet, 1989).

Cell Transfection

Cardiomyocytes were transfected with a mitochondria-targeted cameleon using Effectene (Qiagen, Hilden, Germany) according to the manufacturer's protocol. Experiments were performed 2–3 d later to ensure that mitochondrial targeting was completed (Miyawaki *et al.*, 1997).

Immunoprecipitation of Proteins and Western Blotting

Whole-cell lysates were subjected to immunoprecipitation (Puceat and Vassort, 1996). Samples were run in 5% SDS PAGE and electrophoretically transferred to a nitrocellulose filter. Blots were treated as described previously (Puceat and Vassort, 1996) and probed with the antibody recognizing the protein of interest and a secondary peroxidase-conjugated antibody. Proteins were revealed using ECL reagent. Bands on films were quantified by an imaging system (SCION NIH IMAGE software; Bethesda, MD). The anti-IP_3 receptor type I antiserum was raised against the 14 C-terminal amino acid residues (GHPPHMNVNPQQPA), and the anti-IP_3 receptor type II antisera were raised against the 13 C-terminal amino acids (SNTPHVNHHMPPH [Parys *et al.*, 1995]) or against the sequence of 16 C-terminal amino acids (FLGSNTPHENHHMPPH).

Immunostaining

Cells were fixed with 3% paraformaldehyde, immunostained with an affinity-purified anti-IP_3R antibody directed against the N-terminal domain of the IP_3RI (AA 337–349, QDASRSRLRNAQE), the anti-IP_3RII antiserum, an anti-calreticulin, or monoclonal anti-RyR2 antibodies and a secondary fluorescein-conjugated antibody, and imaged by confocal microscopy (Puceat *et al.*, 1995).

Microinjection, Confocal Microscopy, and Cell Ca^{2+} Imaging

Microinjection of neonatal cells was performed as described (Puceat *et al.*, 1998). The concentrations of Fluo3, Ca^{2+} Green, caged IP_3, and Ca^{2+}-saturated caged EGTA in the pipette were 2.5, 2.5, 2, and 5 mM, respectively. Noninjected cells were loaded with 3 μM Fluo3 AM for 20 min at room temperature. Cells were transferred to the stage of an epifluorescence microscope (Zeiss, Thornwood, NY) and superfused with a medium containing (in mM): HEPES 20, NaCl 117, KCl 5.7, NaH_2PO_4 1.2, $NaHCO_3$ 4.4, $MgCl_2$ 1.7, and $CaCl_2$ 1.8. In Na^+ and Ca^{2+}-free solution, 1 mM EGTA was added, LiCl replaced NaCl, and NaH_2PO_4 and $NaHCO_3$ were omitted. Cardiomyocytes were imaged with a Zeiss LSM-410 or LSM-510 laser-scanning microscope (Thornwood, NY) using the 488-nm line of an argon/krypton laser. Fluo3 or Ca^{2+} Green emission fluorescence was recorded through a dichroic mirror (cutoff of 510 nm) and a long-pass emission filter (cutoff of 520 nm) as described (Jaconi *et al.*, 1997). Caged compounds were photoreleased by simultaneously scanning the field of interest with the 363-nm line of an argon/UV laser. The scan duration was determined using a Uniblitz shutter (Vincent Associates, New York, NY) placed in the UV path. The power of the UV laser beam was set to 200–250 μW, as measured at the aperture of the 40× objective. Exposure of cardiomyocytes to several UV laser scans (for 0.1 or 1 s) in the absence of a caged compound did not affect $[Ca^{2+}]_i$, indicating that UV light does not damage cells under this condition. For localized and spatially restricted IP_3 and Ca^{2+} uncaging, a Zeiss LSM-510 microscope was used. Uncaging was performed in a region of "bleaching" drawn freehand around the nucleus of a cell. Uncaging was performed by bleaching (UV scanning) the area during one scan (100 ms) of concomitant argon/krypton and UV lasers. Experiments were performed at 20 ± 2°C. Sequences of digitized images were background-subtracted and analyzed using the ANALYZE software (Mayo Foundation, Rochester, MN). In experiments designed to look at localized Ca^{2+} events, the first image of the series (Fo) was first subtracted from the following. Then each image of the series was divided by the first image (ΔF/Fo). This normalization of images allows one to take into account the local inhomogeneities of Fluo3. Caged EGTA saturated with Ca^{2+} (Molecular Probes, Eugene, OR) was used to release Ca^{2+} in a locally restricted perinuclear area.

Microspectrofluorimetry and Imaging of Cell Ca^{2+} and Membrane Potential

A cell-imaging system was used to record fluorescence from Fluo3-injected cells. The field was illuminated at 485 ± 22 nm with a xenon lamp. Images were recorded at 530 nm using a charge-coupled device (CCD) camera (Hamamatsu, Bridgewater, NJ) and digitized on-line by computer (Argus software; Hamamatsu). Experiments were performed at 35 ± 2°C in cardiomyocytes microinjected using an Eppendorf (Hamburg, Germany) transjector. The intrapipette concentrations were as follows: Fluo3 2.5 mM; heparin 5 mg/ml; anti-PLCγ antibody (Roche *et al.*, 1996), affinity-purified IgG, or anti-*yes*·6 antibody at 500 μg/ml in KCl 150 mM; EGTA 0.025 mM; EDTA 0.1 mM; and piperazine-*N*,*N*′-bis(2-ethanesulfonic acid) 1 mM (pH 7.2). Wild-type (wt) and mutated (mt) glutathione-*S*-transferase (GST) fusion proteins composed of the two SH2 domains of PLCγ (N- and C-terminal) were prepared as described (Carroll *et al.*, 1997). In the mutated protein, a lysine was replaced by an arginine in the conserved FLVR sequence of the SH2 domains, eliminating binding of the target tyrosine kinase. Fusion proteins were separately injected together with Fluo3 into cardiomyocytes using an intrapipette concentration of 2 mg/ml. IP_3-5-phosphatase was injected at an intrapipette activity of 10 μmol·min^{-1}·ml^{-1} of injection buffer supplemented with 2.5 mM $MgCl_2$. In experiments requiring rapid acquisition, we used a photomultiplier tube (Nikon, Garden

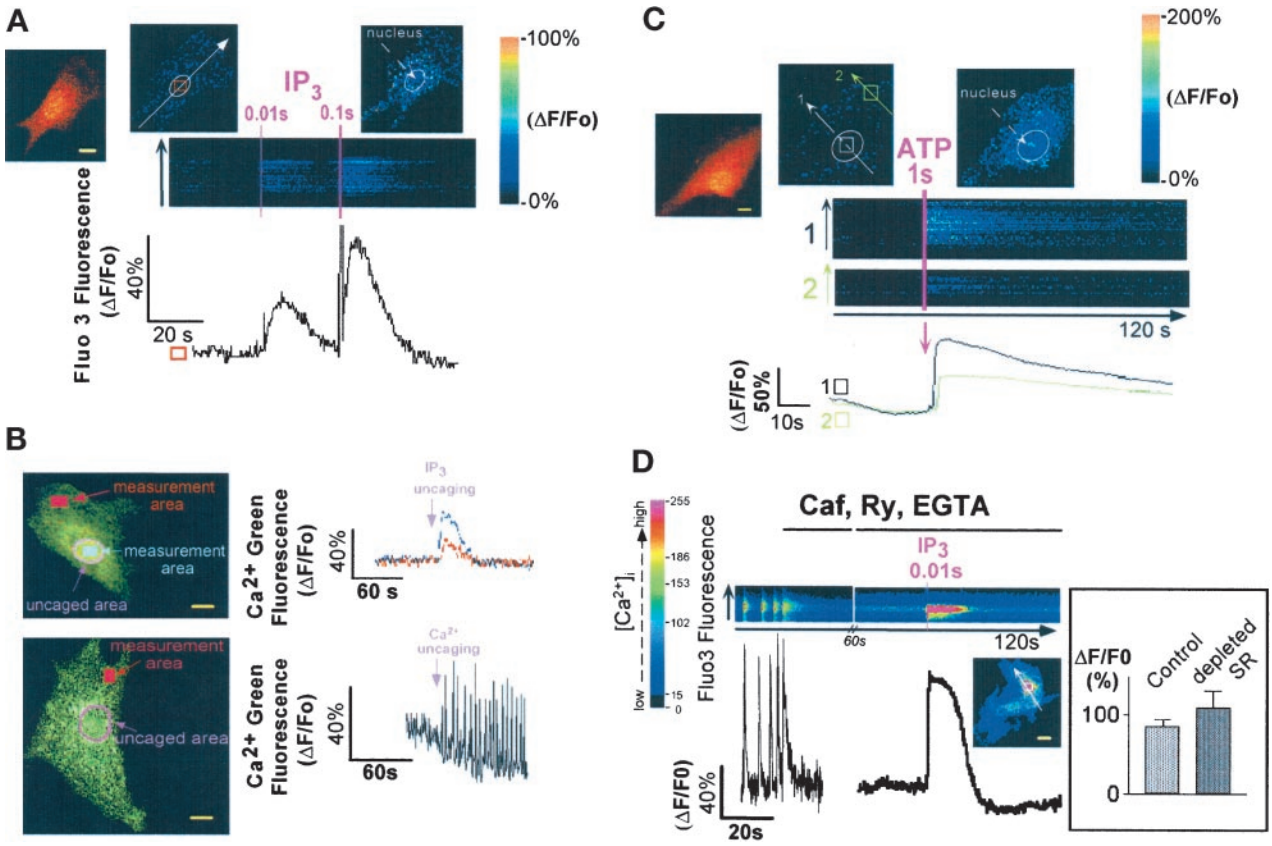

Figure 1. Localized changes of $[Ca^{2+}]_i$ in neonatal rat cardiomyocytes after photorelease of intracellular caged IP_3 or extracellular caged ATP. (A) Caged IP_3 was microinjected together with Fluo3 into cardiomyocytes, and IP_3 was photoreleased by simultaneously scanning the optical field of the microscope with a UV laser beam. The duration of the scans (pink lines) is indicated at the top of the images. Images were acquired every 200–300 ms, and line scan images were built by setting a line crossing the cell (white arrow). The two images on top of the line scan show the cell (normalized fluorescence) before (middle) and after (right) IP_3 release. The left cell image shows the Fluo3-loaded cell, after IP_3 release. The graph represents changes in Fluo3 fluorescence in a region of interest shown by the square. Results (graph and images) are expressed as changes in fluorescence divided by the resting fluorescence ($\Delta F/Fo$) to normalize the Fluo3 signals with the basal fluorescence. Similar results were obtained in seven cells. (B) IP_3 (top) or Ca^{2+} (bottom) was photoreleased around the nucleus (pink area) from caged IP_3 or Ca^{2+}-saturated caged EGTA microinjected together with Ca^{2+} Green into cardiac cells. Note that Ca^{2+} was released to the same extent as the one released by IP_3. The images were acquired using the LSM-510 confocal microscope (confocal section of 0.8 μm). The graphs show the intensity of the Ca^{2+} Green signal after normalization ($\Delta F/Fo$) in different regions of interest (measurement areas). The panel is representative of at least seven experiments. (C) Cardiomyocytes were bathed in a Ca^{2+}-free solution containing 1 mM caged ATP. ATP was photoreleased by a UV laser scan. Line scan images were built as described above. The two normalized images on top of the line scan show the cell before (middle) and after (right) ATP uncaging in the surrounding medium. The left cell image shows the Fluo3-loaded cell, after ATP release. The image is representative of at least five experiments. (D) A spontaneously beating cell was stopped by the addition of 10 mM caffeine (Caf) in the presence of 100 μM ryanodine (Ry) and 1 mM EGTA. Then after 1 min, IP_3 was photoreleased. The graph ($\Delta F/Fo$) shows the release of Ca^{2+} induced by IP_3 in the region of interest delimited by the square; the line scan image was built as described above. Inset, the bar graph represents the changes in Fluo3 fluorescence induced by IP_3 (10-ms UV laser scan), measured in an ROI including the whole cell, under control conditions (1.8 mM extracellular Ca^{2+}) or after Ca^{2+} depletion of the SR (by application of 10 mM caffeine) followed by superfusion of the cell with ryanodine and EGTA ($n = 7$). Yellow bars, 10 μm.

City, NY) coupled to a microscope. The fluorescence signal was digitized and sampled on a computer using Axotape software (Axon Instruments, Foster City, CA).

Cell membrane potential was measured in cells microinjected with JPW1114 (3 mg/ml in the pipette) (Antic and Zecevic, 1995). Cells were microinjected and fluorescence was measured with a photomultiplier tube at 640 ± 20 nm using a DM 580 dichroic mirror (Nikon) and an excitation wavelength at 514 ± 10 nm. When both membrane potential and $[Ca^{2+}]$ were measured, both JPW1114 (3 mg/ml) and Fluo3 (2.5 mM) were injected. The sets of a dichroic mirror and filters mounted on a slider under the objectives of a Nikon microscope were manually switched to allow alternative monitoring of JPW1114 or Fluo3 fluorescence. The JPW1114 fluorescence signal acquired by the computer was filtered, by averaging adjacent data points using the Origin microcal software (Microcal, Northampton, MA). The signal was calibrated by the addition of external KCl to a cell, and the membrane potential was calculated in accord with the Nernst equation (Puceat *et al.*, 1991).

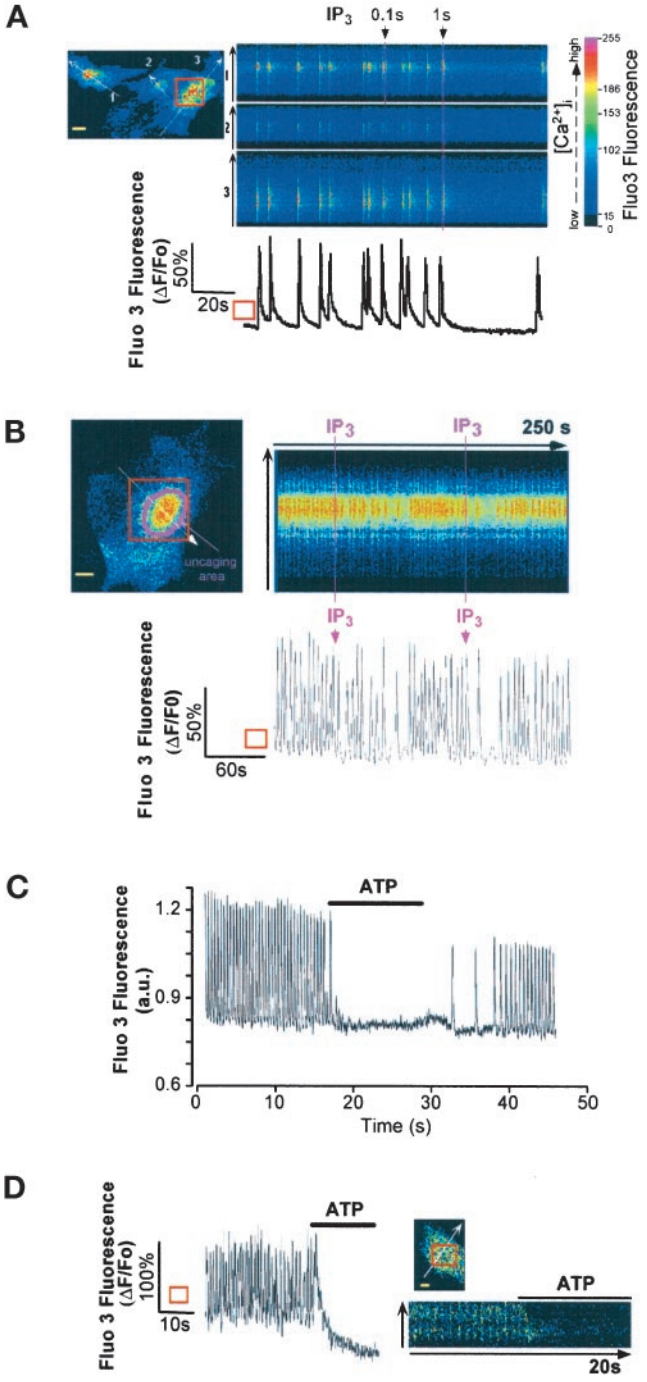

Figure 2. (A) IP_3 stops or slows Ca^{2+} spiking. Spontaneously beating cardiomyocytes injected with Fluo3 and caged IP_3 were bathed in Ca^{2+}-containing solution. IP_3 was photoreleased by scanning the optical field with a UV laser beam (100 ms) that reached the cells at resting $[Ca^{2+}]_i$ (first UV exposure) or at the peak of the Ca^{2+} transient (second UV exposure). The panel is representative of six experiments. (B) Spontaneously beating cardiomyocytes injected with Fluo3 and caged IP_3 were bathed in Ca^{2+}-containing solution. IP_3 was locally photoreleased around the nucleus by "bleaching" (100 ms) with a UV laser beam the uncaging area. The panel is representative of three experiments. The graphs in A and B are expressed as ΔF/Fo and represent changes in Fluo3 fluorescence in the ROI (square). (C and D) A spontaneously Ca^{2+}-spiking cell loaded with Fluo3 was superfused with 20 μM ATP (indicated by horizontal bar), and Fluo3 fluorescence was monitored with a photomultiplier (C) or by imaging the cell by confocal microscopy (optical section of 0.8 μm; D). The line scan (D, right) was built as described in Figure 1. The graph in D is expressed as ΔF/Fo and represents changes in Fluo3 fluorescence in the ROI (square). Bars, 10 μm.

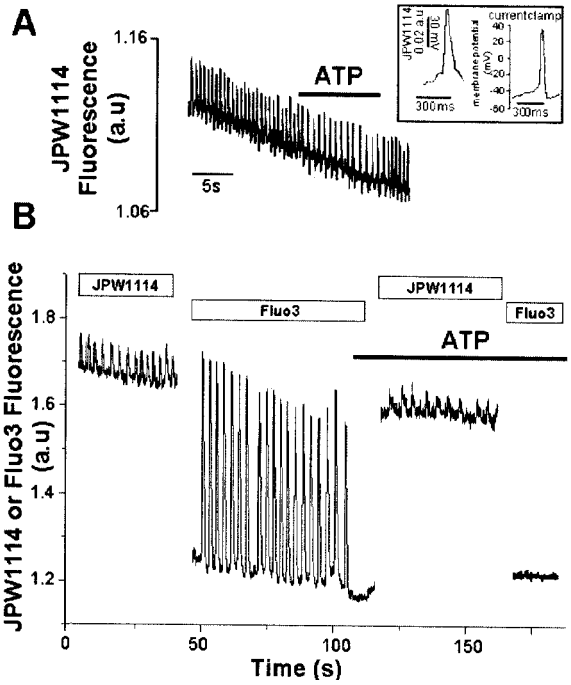

Figure 3. Spontaneous firing of action potentials in neonatal cardiomyocytes. (A and B) Cells were microinjected with JPW1114 (A) or with both JPW1114 and Fluo3 (B). ATP was superfused at a concentration of 20 μM, and changes in fluorescence were recorded by a photomultiplier, digitized, and sampled by a computer. Inset, typical action potentials recorded using JPW1114 or current clamp are shown. The figure is representative of at least six experiments.

Mitochondrial Ca^{2+} and Membrane Potential Measurements

Cells were loaded for 30 min at room temperature with 3 μM Rhod2 AM. The field was illuminated at 514 ± 10 nm (Rhod2) with a xenon lamp. Images were recorded using a 100× objective at 580 nm (Rhod2) using a CCD camera (Hamamatsu) and digitized on-line using a computer (Argus software; Hamamatsu) or a 63× objective using the LSM-510 confocal microscope (optical section of 0.8 μm). Only cells in which Rhod2 was compartmentalized into mitochondrial clusters (as determined by mitotracker staining; Molecular Probes, Portland, OR) were used in the experiments. Regions of interest (ROIs) were set into the center of bright clusters of mitochondria for recording. The position of these ROIs was monitored during the experiment using an off-line analysis (line scan mode using ANALYZE software), and cells in which the mitochondria moved because of their intrinsic motion or of cell contraction were

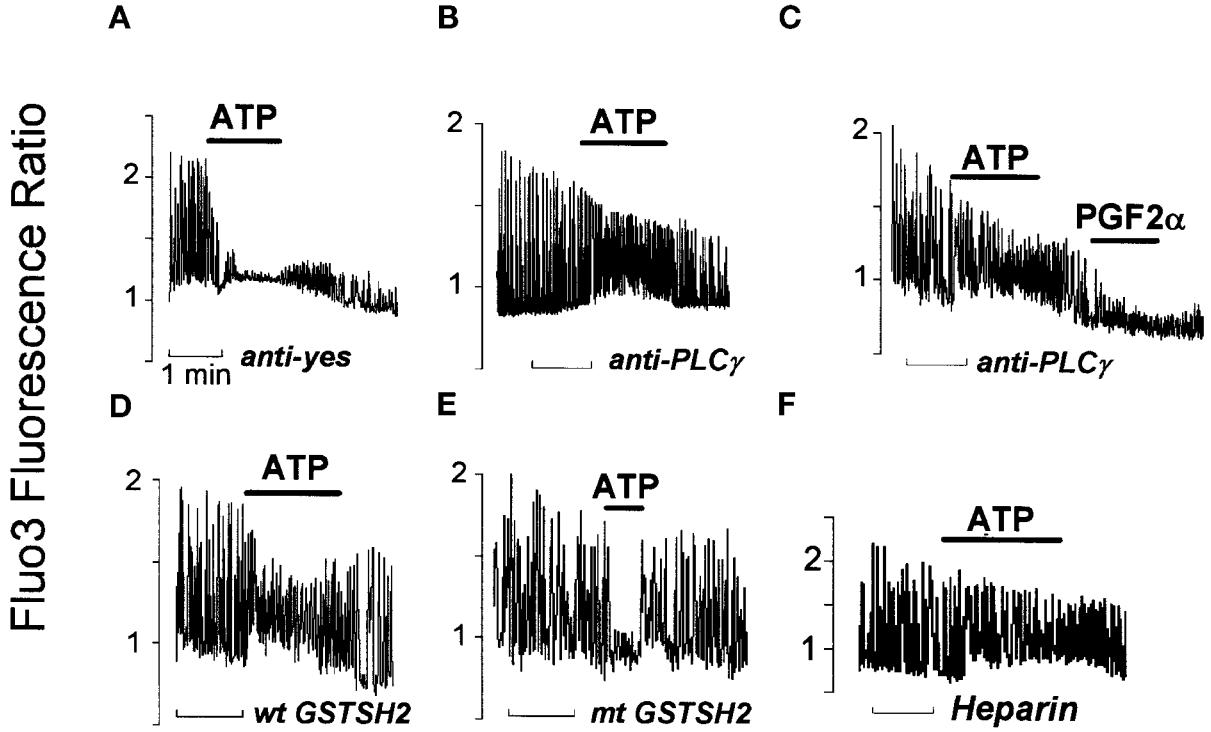

Figure 4. IP_3 generated by PLCγ is required for ATP-induced arrest of Ca^{2+} spiking. Fluo3 was coinjected in cardiomyocytes with an anti-yes antibody (A), an anti-SH2PLCγ antibody (B and C), a wild-type (wt GSTSH2; D) or mutated (mt GSTSH2; E) glutathione-*S*-transferase fusion protein, or heparin (F). The effects of ATP (20 μM) or prostaglandin $F_{2\alpha}$ ($PGF_{2\alpha}$; 1 μM in C) on Ca^{2+} oscillations were tested on spontaneously beating cells. $[Ca^{2+}]_i$ changes were recorded using a CCD camera and the Argus-50 image processor (Hamamatsu). The horizontal bar below each recording indicates the time scale (1 min). The *y*-axes of the graphs represent the Fluo3 fluorescence ratio between each image of the series and the first image acquired at resting $[Ca^{2+}]_i$ as calculated by the Argus-50 software. Three to four images were acquired per second. The number of experiments performed in each experimental condition is indicated in the text. In this series of experiments, a block in Ca^{2+} oscillations was taken as a readout of the ATP effect because the limited time acquisition of the camera did not allow for an accurate estimation of the spiking rate.

discarded. Cells were also loaded with TMRM (3 μM) and Fluo3 (3 μM) for 20 min and then washed. Cells were imaged by confocal microscopy using the 488-nm line of an argon laser and a cutoff dichroic mirror of 560 nm. Fluorescence was recorded using two photomultipliers and emission filters of 522DF35 for Fluo3 and 605DF32 for TMRM (Nikon). A focal plane of 0.8 μm was selected in these experiments. Experiments were analyzed using the ANALYZE software (Mayo Foundation). In experiments using a mitochondria-targeted cameleon, cells were illuminated at 430 nm, and fluorescence was recorded with a CCD camera at 480 ± 30 and 535 ± 25 nm. Images were acquired every 3 s. The ratio of images at 535 nm/480 nm was calculated off-line after background subtraction, by the software Metamorph (Universal Imaging, West Chester, PA), and used as an index of mitochondrial Ca^{2+}changes. Only cells in which the cameleon was fully targeted into mitochondria were used.

RESULTS

IP_3 Induces Spatially Restricted Intracellular Ca^{2+} Release from a Caffeine- and Ryanodine-insensitive Pool

Cardiomyocytes, plated at low density, feature a steady resting membrane potential associated with an inward-rectifying I_{K1} current (Maltsev *et al.*, 1994). A brief UV laser scan, aimed at a portion of a quiescent cell microinjected with both the Ca^{2+}-sensitive probe Fluo3 and caged IP_3, triggered the photorelease of IP_3. This, in turn, induced a fast increase in the intracellular Ca^{2+} concentration ($[Ca^{2+}]_i$). Longer laser scans (illuminating cells for several consecutive frames) uncaged a larger amount of IP_3 and induced a larger Ca^{2+} transient (Figure 1A). IP_3-induced Ca^{2+} release was confined to the perinuclear area of cardiomyocytes and did not trigger regenerative waves through the cytosol, nor did it induce CICR from other cellular compartments as observed recently in neurons (Finch and Augustine, 1998) (Figure 1A). Photorelease of IP_3 in a localized region of interest set around the nucleus further revealed the limited diffusion pattern of Ca^{2+} released by IP_3. The Ca^{2+} signal was much smaller and delayed a few micrometers away from the site of IP_3 release. In contrast, Ca^{2+} photoreleased in the perinuclear area from Ca^{2+}-saturated caged EGTA triggered Ca^{2+}-induced CICR, even far beyond the site of Ca^{2+} release (Figure 1B).

The purinergic agonist ATP, known to generate IP_3, also induced the release of intracellular Ca^{2+} when quickly photoreleased from its caged precursor in a Ca^{2+}-free

extracellular environment of quiescent cardiomyocytes. Similarly to IP_3-triggered Ca^{2+} release, the ATP-induced Ca^{2+} release was spatially localized to the perinuclear region without triggering Ca^{2+} oscillations in other cellular domains (Figure 1C). Ca^{2+} release was still observed with the same magnitude (Figure 1D, inset) when IP_3 or ATP was uncaged in or around cells bathed in Ca^{2+}-free solution after a fast application of caffeine (10 mM) in the presence of ryanodine (100 μM). This experimental condition was used to deplete Ca^{2+} from the SR and to prevent Ca^{2+} store refilling (Figure 1D). Thus, IP_3 releases Ca^{2+} within a spatially restricted area from a ryanodine- and caffeine-insensitive pool.

IP_3 Arrests Spontaneous Ca^{2+} Spikes

Cardiomyocytes plated at high density exhibited spontaneous beating associated with Ca^{2+} firing after development of pacemaker currents (Gomez *et al.*, 1994; Maltsev *et al.*, 1994). Caged IP_3, microinjected in such cells and photoreleased by a UV laser scan, resulted in a dramatic slowing or transient arrest of Ca^{2+} oscillations at diastolic Ca^{2+} levels (Figure 2A). The effect of IP_3 was dependent on the duration of cell exposure to the uncaging UV light and, thus, to the amount and/or site of released IP_3. A local IP_3 photorelease around the nucleus also dramatically and transiently decreased the rate of Ca^{2+} spiking (Figure 2B). Superfusion of cells with ATP slowed the rate (in 45% of cells) (our unpublished results) or abolished (in 55% of cells) spontaneous Ca^{2+} oscillations (Figure 2C). A similar effect was observed when the related homologue UTP, an agonist selective for purinergic P2Y receptors, was used instead of ATP that binds both P2X and P2Y receptors (our unpublished results). Confocal imaging of a Ca^{2+}-oscillating cell revealed that the purinergic agonist first induced transient intracellular Ca^{2+} release, mainly localized around the nucleus, which preceded the arrest of Ca^{2+} oscillations (Figure 2D).

In principle, an arrest in cardiac automatic activity may result from perturbations in cell excitability and thus in membrane ionic currents. This prompted us to monitor the effect of ATP on the spontaneous firing of action potentials in automatic cardiomyocytes injected with the potential sensitive probe JPW1114 (Antic and Zecevic, 1995). Action potentials recorded with this probe featured a shape and time course similar to the ones recorded using the current-clamp technique (Figure 3A, inset). The purinergic agonist slowed but never stopped spontaneous action potentials as expected from the lack of effect of IP_3 or ATP on Ca^{2+} or K^+ currents in these cells (our unpublished results). No change in resting membrane potential was observed upon application of ATP (Figure 3A). We then alternatively recorded action potentials and cytosolic Ca^{2+} in the same single cell, microinjected with both JPW1114 and Fluo3. Although ATP stopped repetitive Ca^{2+} spiking, action potentials were still firing although at a lower frequency (Figure 3B, 52 ± 6% of control frequency; n = 8) as observed previously (Figure 3A). This excludes the possibility that a change in membrane potential that may result from a modulation of depolarizing ionic conductances such as the ATP-gated P2X channel (Vassort *et al.*, 1994) could account for the purinergic effect on Ca^{2+} spiking. A direct action on intracellular Ca^{2+} homeostasis is thus more likely to account for the modulation in Ca^{2+} spiking.

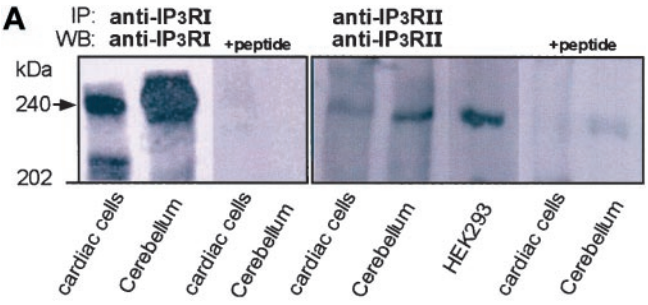

Figure 5. IP_3RIs are localized in a caffeine- and ryanodine-insensitive Ca^{2+} store. (A) IP_3RIs and IP_3RIIs immunoprecipitated from cultured cardiomyocytes, cerebellum, or human embryonic kidney 293 (HEK293) cells using specific antisera. We used 1.5, 0.3, and 1 mg of cardiac whole-cell lysate, cerebellum homogenate, and HEK293 whole-cell lysate proteins, respectively, in this experiment. After immunoprecipitation (IP), SDS-PAGE, and Western blotting (WB), the blots were probed with the respective specific affinity-purified antibodies. The peptides used to raise the antibodies were used in competition assay. Two different anti-IP_3RII antisera were tested, giving the same results. No proteins were immunoprecipitated using the preimmune IP_3RI or IP_3RII antisera. The blot is representative of four experiments. (B) Immunofluorescence labeling and confocal imaging of neonatal rat cardiac cells using an affinity-purified anti-IP_3RI antibody (raised against the N-terminal AA 337–349; I), an anti-calreticulin antibody (II), green mitotracker (III), green mitotracker (green staining) together with an affinity-purified anti-IP_3RI antibody (red staining; IV), or an anti-RyR 2 receptor monoclonal antibody (Affinity Bioreagents, Golden, CO; V). IP_3RI and calreticulin stainings were revealed by a secondary FITC-conjugated anti-rabbit IgG, and RyR was revealed by a TRITC-conjugated anti-mouse IgG except in IV where a TRITC-conjugated anti-rabbit IgG was used to reveal IP_3Rs in green mitotracker-loaded cells. No staining was observed when cells were incubated with only the secondary antibody. A nuclear localization of calreticulin has been observed recently in different cell lines (Roderick *et al.*, 1997). The labeling was observed by confocal microscopy using a Bio-Rad MRC1024 microscope (Richmond, CA) and a 60× magnification objective. The images show a 0.5-μm optical section using a zoom of 1 in III (left), 1.5 in I, II, and III (right), and 2 in IV. Bars, 10 μm.

Furthermore, we isolated Purkinje cells (Scamps and Carmeliet, 1989) of the cardiac conduction system rich in IP_3Rs (Gorza *et al.*, 1993). Membrane depolarization–induced Ca^{2+} spiking was triggered by external pacing at 1 Hz. Application of ATP dramatically decreased Ca^{2+} transients or stopped Ca^{2+} spiking of these cells (n = 5 cells). This effect was no longer observed in Purkinje cells treated with neomycin or U79122, two inhibitors of PLCs (n = 5 cells) (our unpublished results).

IP_3-induced Ca^{2+} Release Is Required for ATP-induced Arrest of Ca^{2+} Spiking

ATP, unlike most other agonists, generates IP_3 predominantly, if not exclusively, via activation of the tyrosine kinase–regulated PLCγ (Puceat and Vassort, 1996). To disrupt the purinergic signal transduction pathway that leads to IP_3 generation, we microinjected neonatal cardiomyocytes with a blocking anti-PLCγ antibody raised against the SH2 domains of the lipase (Roche *et al.*, 1996). Affinity-purified

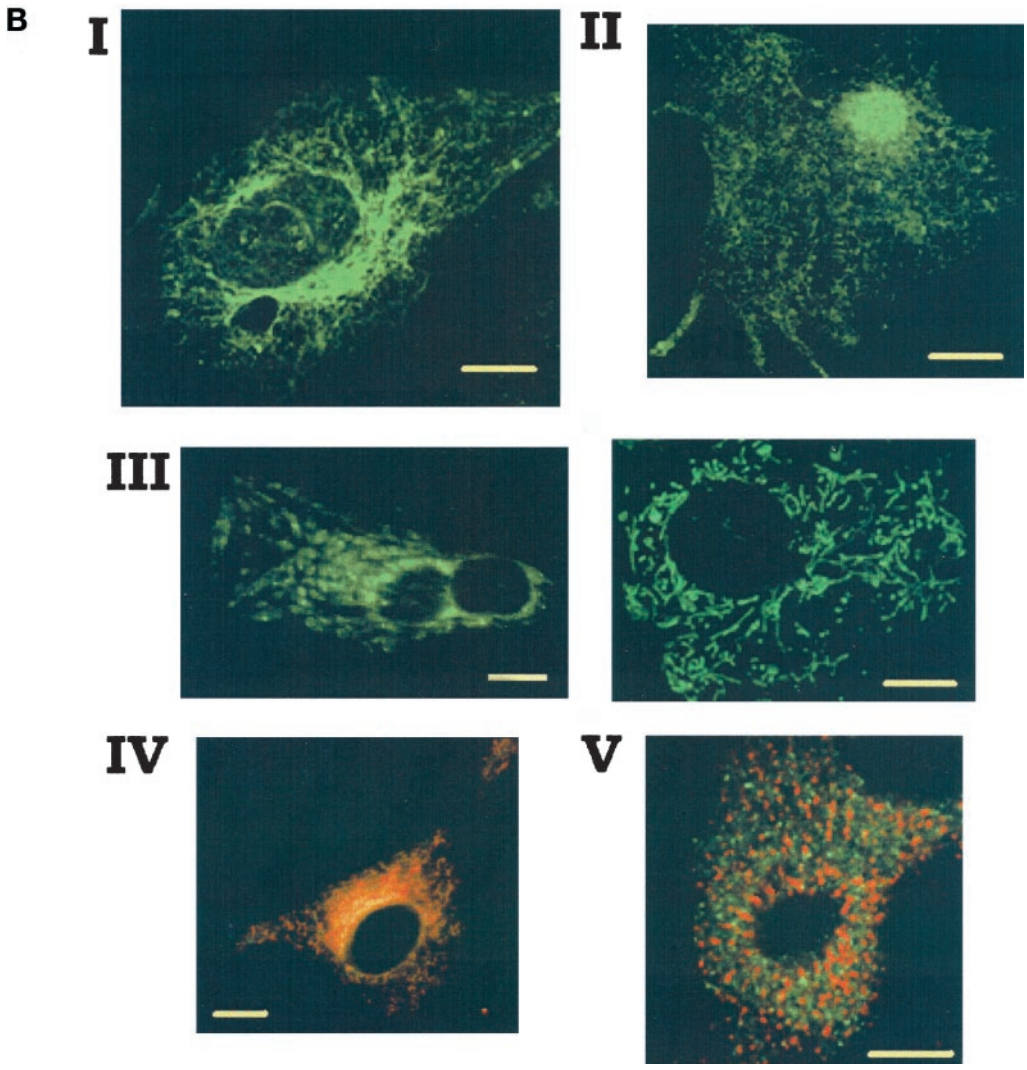

Figure 5 (cont).

rabbit IgG or an antibody directed against the *yes* tyrosine kinase, not expressed in cardiomyocytes, was microinjected as a control antibody. In these cells, application of 20 μM ATP rapidly abolished spontaneous Ca^{2+} spiking as observed in noninjected cells (Figure 4A), indicating that microinjection of antibodies did not affect the purinergic response. In anti-PLCγ antibody–injected cells, however, the purine induced an increase in diastolic Ca^{2+} associated with a slight decrease in the amplitude of Ca^{2+} oscillations, but in 80% of these cells, Ca^{2+} oscillations were still observed, and their frequency was increased (12 out of 15 cells) (Figure 4B). In contrast to ATP, $PGF_{2\alpha}$ generates IP_3 via activation of the Gq-coupled PLCβ (Adams *et al.*, 1998), an isoform that lacks the SH2 domain. Like ATP, $PGF_{2\alpha}$ blocked the Ca^{2+} firing of cardiomyocytes, but this was not blocked by the anti-PLCγ antibody raised against the SH2 domain, demonstrating the specificity of the antibody (Figure 4C). A GST fusion protein, composed of the two SH2 domains of PLCγ (at the N- and C-terminals), acts as a "dominant-negative" protein (GSTSH2) (Carroll *et al.*, 1997) when microinjected in cardiomyocytes and prevents PLCγ phosphorylation and thus its activation. The wild-type GSTSH2 prevented ATP from abolishing spontaneous Ca^{2+} spiking in 19 out of 23 microinjected cardiomyocytes, with ATP inducing an increase in diastolic Ca^{2+} in these cells (Figure 4D). In cells microinjected with the mutated GSTSH2 (Carroll *et al.*, 1997), ATP stopped or significantly decreased both the amplitude and the frequency of oscillations (in 20 out of 22 cells) (Figure 4E). In heparin-injected cells in which IP_3 cannot bind its receptor, ATP increased diastolic Ca^{2+} ($n = 9$) but did not stop spontaneous Ca^{2+} spiking (Figure 4F). A lack of effect of ATP was also observed in cells microinjected with the IP_3-5-phosphatase that accelerates IP_3 hydrolysis or with an anti-Cst1 antibody that prevents activation of the tyrosine kinase–dependent pathway (Puceat *et al.*, 1998) (our unpublished results).

Intracellular Localization and Properties of the IP_3-sensitive Intracellular Ca^{2+} Pool

Immunoprecipitation and Western blotting of IP_3Rs using isoform-specific antibodies revealed that neonatal rat cardiomyocytes express both IP_3R type I and II proteins migrating with an apparent molecular mass of 240 kDa, as expected for IP_3Rs (Mikoshiba *et al.*, 1994). The specificity of the antibodies used was confirmed by competition using respective immunizing peptides (Figure 5A).

Confocal micrographs of cells immunostained with a specific anti-IP_3RI antibody revealed labeling around the nucleus that projected as a reticular network toward the cell periphery (Figure 5B, I). This network was however less dense than that revealed by an anti-calreticulin antibody that stains both endoplasmic reticulum (ER) and SR (Figure 5B, II). Staining of cells preincubated with green mitotracker revealed a filamentous (Figure 5B, III, right image) or a more clustered (Figure 5B, III, left image) distribution of mitochondria. Dual staining of cells with both mitotracker and purified anti-IP3RI antibody showed a distribution of IP3Rs very close to the one of mitochondria, specifically around the nucleus (Figure 5B, IV). Immunocytochemistry failed to detect IP_3RII probably because of the low level of expression of this isoform in cardiomyocytes as assessed by immunoprecipitation (Figure 5A). Double immunostaining of cells with both the anti-IP_3RI and anti-RyR antibodies clearly showed that both receptors were not colocalized in cardiomyocytes (Figure 5B, V).

Mechanism of IP_3-induced Abolishment of Spontaneous Ca^{2+} Spiking

A major question is how IP_3-induced Ca^{2+} release may affect CICR originating from the SR in spontaneously Ca^{2+}-spiking cells. Recent studies have shown in noncardiac cells a close interaction between the IP_3-sensitive ER and mitochondria (Rizzuto *et al.*, 1993, 1998; Loew *et al.*, 1994; Babcock *et al.*, 1997). Furthermore, these organelles are known to take up Ca^{2+} released on a beat-to-beat basis by the SR in the heart (Chacon *et al.*, 1996; Duchen *et al.*, 1998; Ohata *et al.*, 1998). Parallel experiments showed that Ca^{2+} sequestration in mitochondria using the inhibitor of the transient permeability pore cyclosporin A also slowed the rate and stopped cell Ca^{2+} spiking (Figure 6A). We thus designed experiments to test whether cardiac mitochondria could sequester both Ca^{2+} released by the IP_3-sensitive store and Ca^{2+} cycling from and into the SR, depleting the caffeine-sensitive store (Figure 1A). First, SR Ca^{2+} content was estimated by caffeine-triggered Ca^{2+} release. Consecutive applications of caffeine shortly after stopping Ca^{2+} spiking of cells with a Na^+- and Ca^{2+}-free medium that prevents the activity of the Na^+/Ca^{2+} exchanger triggered a Ca^{2+} release of similar magnitude (Figure 6B). However, upon stopping Ca^{2+} spiking with extracellular ATP, the magnitude of the caffeine-induced Ca^{2+} release was significantly decreased (Figure 6C, bottom; n = 9). A similar effect was observed when $PGF2_\alpha$ was used instead of ATP to generate cytosolic IP_3 (n = 3 cells) (our unpublished results).

To determine whether, in cardiomyocytes, mitochondria distributed in the close vicinity of IP_3Rs (Figure 5B I, III, and IV) sense Ca^{2+} released by IP_3, cells were first loaded with Rhod2, a mitochondrial Ca^{2+}-sensitive probe. Purinergic stimulation of cells induced a rapid and transient mitochondrial Ca^{2+} uptake (Figure 7A, top left and bottom). These changes were not observed in cells in which ATP-induced IP_3 formation was inhibited by pretreatment for 30 min with 2 mM neomycin (n = 3 cells and 17 mitochondrial clusters), 10 μM U79122 (n = 4 cells and 22 mitochondrial clusters), or 20 μg/ml genistein (n = 3 cells and 21 mitochondrial clusters) or in cells microinjected with a blocking anti-PLCγ antibody (n = 13 cells and 65 mitochondrial clusters) (Figure 7A, top right). Nevertheless, the mitochondrial uncoupler FCCP, which collapses the mitochondrial potential and reverses the activity of the Ca^{2+} uniporter (Kroner, 1992), routinely released Ca^{2+} from the organelles as observed previously in many other cell types (Babcock *et al.*, 1997; Ichas *et al.*, 1997; Boitier *et al.*, 1999; Hajnoczky *et al.*, 1999). FCCP further prevented the ATP-induced mitochondrial Ca^{2+} loading (our unpublished results). Altogether, these data demonstrate the requirement of IP_3 in the purinergic effect on the rate of cell Ca^{2+} spiking. Localized uncaging of IP_3 around the nucleus more directly showed, in Ca^{2+} Green- and Rhod2-loaded cells, that mitochondria pump Ca^{2+} released by IP_3 (Figure 7B). In contrast, global Ca^{2+} release from the SR by caffeine did not trigger any significant increase in Rhod2 fluorescence, whereas ATP applied to the same cell did (Figure 7C).

To investigate further the privileged transfer of Ca^{2+} from IP_3-sensitive pools to mitochondria, cardiomyocytes were transfected with a mitochondria-targeted cameleon (Miyawaki *et al.*, 1997). Figure 7D shows that the distribution of the cameleon is comparable with the one of Rhod2 and mitotracker. Addition of ATP to a cameleon-expressing cell induced an increase in mitochondrial Ca^{2+} as observed previously using Rhod2. Caffeine slightly decreased mitochondrial Ca^{2+}, whereas addition of thapsigargin, a Ca^{2+} ATPase inhibitor that further empties caffeine-insensitive pools, did not affect mitochondrial Ca^{2+} fluxes. Addition of 5 mM Ca^{2+} and ionomycin significantly increased mitochondrial Ca^{2+} (Figure 7D, top). FFCP quickly released Ca^{2+} from mitochondria, confirming the targeting of the cameleon into the organelles (Figure 7D, bottom).

Changes in mitochondrial membrane potential reflect Ca^{2+} movements across the membrane of the organelle (Duchen *et al.*, 1998). In cells loaded with the mitochondrial potentiometric dye TMRM and imaged by confocal microscopy, ATP triggered a transient quenching of the fluorescence, whereas FCCP that leads to a complete dissipation of the mitochondrial potential induced sustained and more pronounced quenching of TMRM fluorescence (Figure 8A). Confocal imaging of cells coloaded with TMRM and Fluo3 showed that depolarization of the mitochondrial membrane occurred just before arrest of the Ca^{2+} oscillations induced by extracellular ATP (Figure 8B).

DISCUSSION

IP_3 Affects Ca^{2+} Intracellular Homeostasis

We have uncovered that IP_3, acting within a restricted spatial range, modulates spontaneous autonomic activity of cardiomyocytes

Modulation of the rate of cell Ca^{2+}spiking may arise either from a change in cell membrane excitability or from a change in the Ca^{2+} content of intracellular stores. Alteration

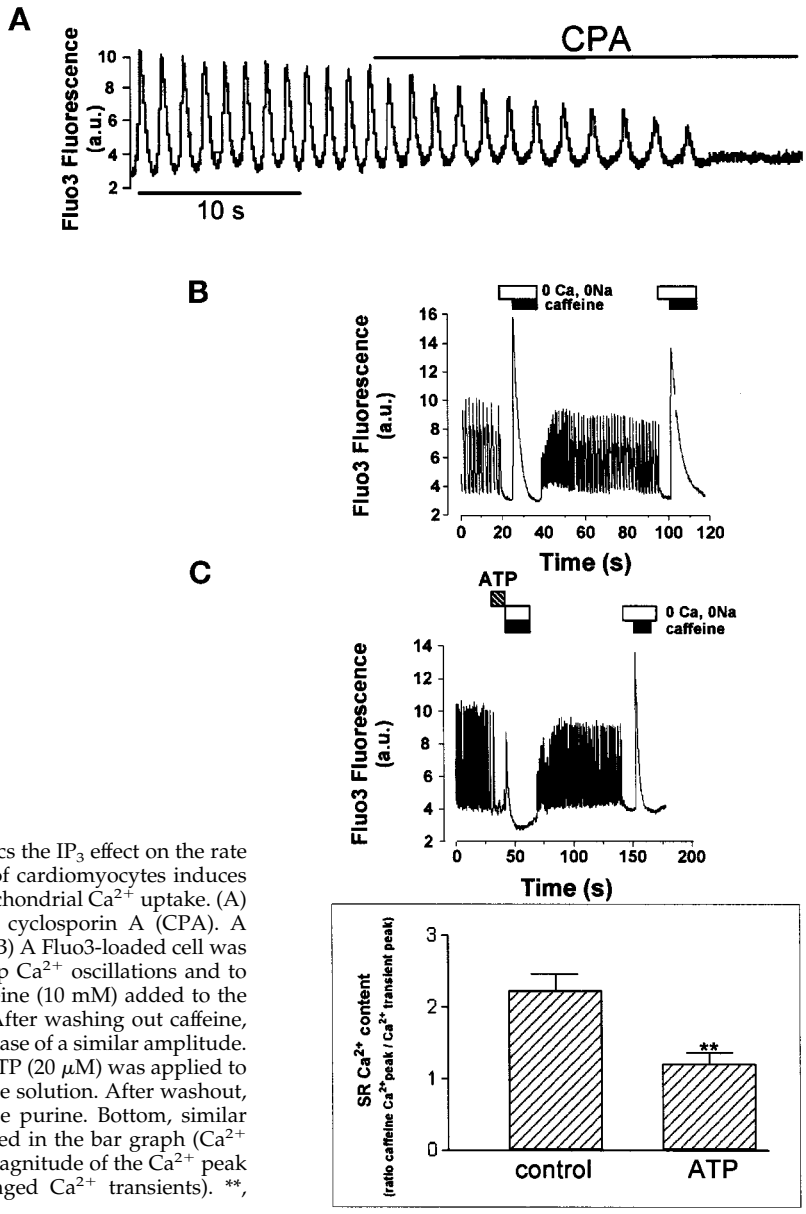

Figure 6. Ca^{2+} sequestration into mitochondria mimics the IP_3 effect on the rate of spontaneous Ca^{2+} spiking. Purinergic stimulation of cardiomyocytes induces Ca^{2+} depletion of the sarcoplasmic reticulum and mitochondrial Ca^{2+} uptake. (A) A Fluo3-loaded cell was superfused with 50 ng/ml cyclosporin A (CPA). A similar effect of CPA was observed in four other cells. (B) A Fluo3-loaded cell was superfused with a Ca^{2+}- and Na^+-free solution to stop Ca^{2+} oscillations and to prevent the activity of the Na^+/Ca^{2+} exchanger. Caffeine (10 mM) added to the Ca^{2+}- and Na^+-free solution was applied to the cell. After washing out caffeine, the same protocol was repeated and triggered Ca^{2+} release of a similar amplitude. Similar results were obtained in seven cells. (C) Top, ATP (20 μM) was applied to the cell. Caffeine was then added in Ca^{2+}- and Na^+-free solution. After washout, the same protocol was repeated in the absence of the purine. Bottom, similar results were observed in at least nine cells and gathered in the bar graph (Ca^{2+} content of the SR was estimated from the ratio of the magnitude of the Ca^{2+} peak triggered by caffeine to the magnitude of the averaged Ca^{2+} transients). **, significantly different ($p \leq 0.01$).

in membrane ion channel conductances by IP_3 generated by the purinergic agonist was discarded because neither the resting membrane potential nor the action potential of cardiomyocytes was affected by purinergic stimulation (Figure 3A). This could be expected from the lack of effect of IP_3 on Ca^{2+} currents (Saeki *et al.*, 1999) or other ionic currents including an iberiotoxin-sensitive Ca^{2+}-activated K^+ current or I_f current (our unpublished results). Furthermore, ATP-induced IP_3 generation stops Ca^{2+}-spiking of paced Purkinje cells, which argues against an IP_3 effect on cell membrane excitability. However, when the IP_3 pathway is disrupted, ATP increases diastolic Ca^{2+} and speeds the rate of Ca^{2+} oscillations (i.e., anti-PLCγ antibody-, GSTSH2-, and heparin-injected cells; Figure 4). This observation might be attributed to an IP_3-independent effect of purinergic stimulation that occurs via P2X receptors (Vassort *et al.*, 1994). This effect is masked when IP_3 is generated by ATP, which further suggests that the P2Y receptor is preferentially activated as reported in transfected cells (Murthy and Makhlouf, 1998). Thus, the effect of IP_3 on autonomic Ca^{2+} spiking can be attributed to a perturbation in intracellular Ca^{2+} homeostasis rather than to a direct change of cell excitability.

The IP_3-sensitive Ca^{2+} Pool: An ER Functionally Distinct from the SR

The main question addressed in this study was the origin of Ca^{2+} released by IP_3. Several findings point to the ER but not to the SR as the IP_3-sensitive Ca^{2+} store. First, spatially

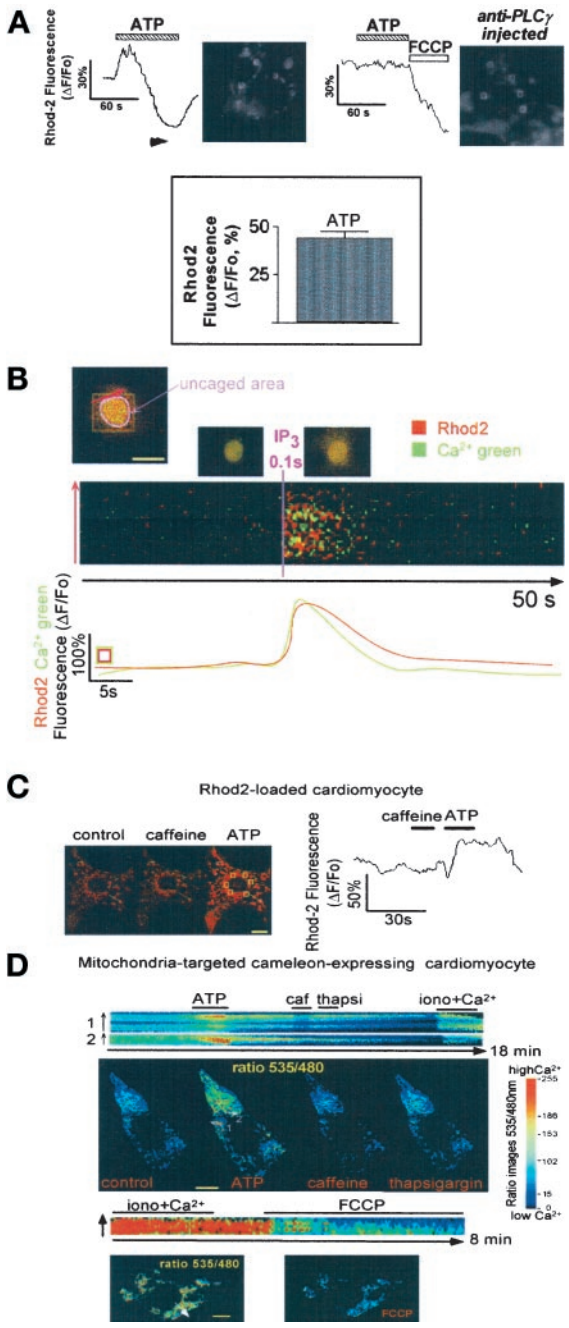

Figure 7. Purinergic stimulation of cardiomyocytes transiently increases mitochondrial Ca^{2+}. (A) Rhod2-loaded cells were superfused with 20 μM ATP (top left). The increase in Rhod2 fluorescence indicates a concomitant rise of mitochondrial Ca^{2+}, whereas a decrease in Rhod2 fluorescence indicates an efflux of Ca^{2+} from mitochondria. The recording is an average of the fluorescence of five mitochondrial clusters around the nuclei of two adjacent beating cells (ROIs delimited by white squares). This average was used to attenuate possible individual changes in the shape of mitochondria. Similar results were observed in 11 cells and expressed in the bar graph (bottom) as the mean ± SEM of $\Delta F/Fo$ measured in 43 mitochondrial clusters from 11 cells. The cell was injected with the anti-PLCγ antibody (500 μg/ml of injection buffer) and then loaded with Rhod2 AM (top right). The recording is an average of the five ROIs delimited by white squares on the cell picture. Three to four images were acquired per second using a CCD camera. (B) Cells were microinjected with caged IP_3 and Ca^{2+} Green and loaded with Rhod2. Cells were imaged by confocal microcopy using a 63× objective. A scanning ROI was set in a small area of the cell that includes the nucleus to get a fast scanning of the UV laser to photorelease IP_3 around the nucleus (pink area). The line scan images were built as described previously (after fluorescence normalization, $\Delta F/Fo$) and established as a line along the nucleus (red line that crosses several clusters of mitochondria). Original fluorescent colors were kept in these experiments. The red fluorescence is generated by Rhod2-loaded mitochondria, whereas the green fluorescence is generated by cytosolic Ca^{2+} Green. The pinhole of the microscope was set to get an optical slice of 2 μm. The yellow fluorescence is generated by an increase in both the mitochondrial and surrounding cytosolic Ca^{2+}, around, above, and/or under the nucleus within the 2-μm confocal plane. This focal plane was selected to avoid artifactual changes in focus. Note that leakage or spatial redistribution of mitochondrial Rhod2 is unlikely because the effect of IP_3 on mitochondrial Ca^{2+} was fully reversible. The graph (bottom) represents the changes in Rhod2 and Ca^{2+} Green fluorescence in the ROI (green/red square) expressed as $\Delta F/Fo$. The images on top of the line scan image show the cell before (middle) and after (right) IP_3 release. The figure is representative of seven separate experiments. (C) Caffeine was added to a Rhod2-loaded cell imaged by confocal microscopy (left). Mitochondrial Ca^{2+} was recorded in the absence or presence of 10 mM caffeine and 20 μM ATP in six different clusters of mitochondria (yellow-squared ROIs). The images show the cell before (control) and after ATP or caffeine application. The yellow lines (intermitochondrial cluster distance) were drawn to check the motion of mitochondria in the course of the experiments (using ANALYZE software). Although mitochondria may move within the cell, such a motion was not recorded within the short time course of our experiments. Cell shortening associated with Ca^{2+} spiking was also limited in the z-direction because of the strong attachment of cells on a laminin-coated coverslip. The graph (right) is an average of the change in Rhod2 fluorescence expressed as $\Delta F/Fo$ in these six ROIs. The figure is representative of seven separate experiments. (D) A cardiomyocyte expressing a mitochondria-targeted cameleon was stimulated by 20 μM ATP or treated with 10 mM caffeine (caf), 1 μM thapsigargin (thapsi) in the presence of 1 mM external Ca^{2+}, or 1 μM ionomycin (iono) in the presence of 5 mM Ca^{2+}. The color images were obtained after making the ratio of the image acquired at 535 nm to the image acquired at 480 nm in the absence or presence of ATP, caffeine, or thapsigargin. As a control for the targeting of the cameleon into mitochondria, a cell was challenged with 10 μM FCCP after superfusion with ionomycin and high Ca^{2+}. The line scan images were obtained by off-line analysis using ANALYZE software as described in the previous figures; lines were set across clusters of mitochondria as indicated by white arrows. Similar data were obtained in at least six cells. Bars, 10 μm.

restricted IP_3-induced Ca^{2+} release is not sensitive to ryanodine or caffeine. Second, IP_3Rs, but not RyRs, feature a perinuclear distribution. Third, perinuclear release of Ca^{2+} triggers a CICR, whereas IP_3 induces a transient single spike (Figure 1B). Furthermore, the kinetics of IP_3-triggered Ca^{2+} release is slower than what would be expected from an SR Ca^{2+} release (Robert *et al.*, 1998) but faster than what may be expected from the Golgi apparatus, a compartment shown recently to be responsive to IP_3 (Pinton *et al.*, 1998; Lin *et al.*, 1999). Finally, ATP or IP_3, but not caffeine, triggered a localized Ca^{2+} release that was sensed by mitochondria. This also

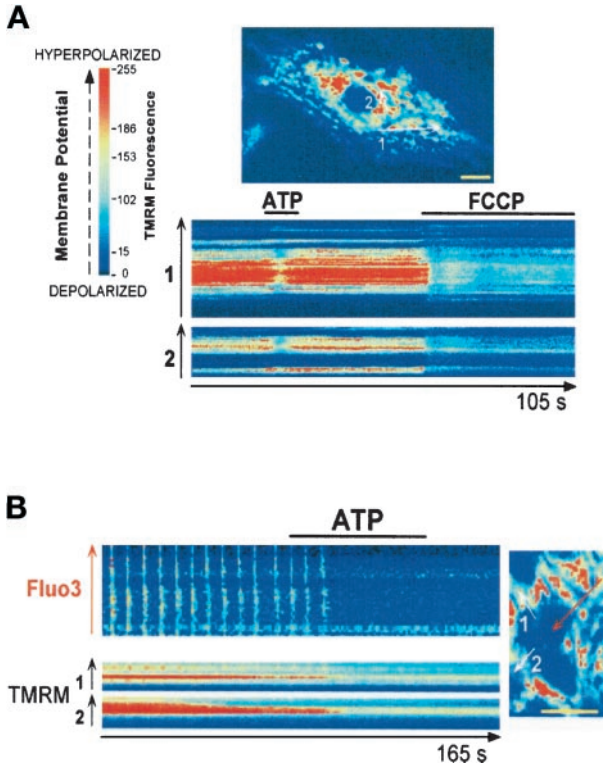

Figure 8. Purinergic stimulation of cells induces a mitochondrial depolarization. Cells were loaded with TMRM (A) or with both TMRM and Fluo3 (B), and changes in the fluorescence of the probes were monitored in the absence or presence of 20 μM ATP using confocal microscopy. Images were acquired every 200–300 ms. Line scan images were built as described in Figure 1. Lines were set across clusters of TMRM-labeled mitochondria or across the cell (Fluo3). FCCP (5 μM) was used as a control to induce a complete dissipation of the mitochondrial potential. The figure is representative of five separate experiments. Bars, 10 μm.

excludes the SR as the IP_3-sensitive Ca^{2+} store. Neonatal rat cardiac cells in culture thus feature an IP_3-sensitive ER pharmacologically and functionally distinct from the SR, as suggested previously for smooth muscle cells (Golovina and Blaustein, 1997) and for cells of the cardiac conduction system (Gorza *et al.*, 1993). Although IP3Rs and RyR do not colocalize (Figure 5), our findings cannot exclude the possibility that the ER and the SR may be two subcompartments of the same store, namely, an ER/SR network

Privileged Ca^{2+} Flow between Mitochondria and ER, a Major Component of the IP_3 Effect on Spontaneous Ca^{2+} Spiking

Despite the absence of IP_3Rs in the SR and the caffeine-insensitive IP_3-dependent Ca^{2+} release, purinergic stimulation slows or stops spontaneous Ca^{2+} spiking after a partial but significant Ca^{2+} depletion of the SR (Figure 6). Participation of mitochondria in the Ca^{2+} homeostasis network (Babcock *et al.*, 1997) as a Ca^{2+} sink, which under specific conditions sequesters Ca^{2+} released by either ER or both ER and SR, may account for this observation.

Mitochondrial Ca^{2+} uptake is a low-affinity (Gunter *et al.*, 1994; Csordas *et al.*, 1999) but a fast process (Sparagna *et al.*, 1995). Evidence supporting the participation of mitochondria in the transient arrest of Ca^{2+} spiking in cardiomyocytes emerges from a series of observations. First, an increase in Rhod2 fluorescence was observed when IP_3 was photoreleased around the nucleus or was generated by purinergic stimulation of cells (Figure 7). Ca^{2+} sequestration into mitochondria upon an IP_3 challenge was further demonstrated in cells expressing a mitochondria-targeted cameleon (Figure 7D). Second, depolarization of mitochondria clustered around the nucleus in the vicinity of the ER coincides with the arrest in cytosolic Ca^{2+} oscillations, both triggered by ATP (Figure 8). Finally, cyclosporin A, which elicits a Ca^{2+} load of mitochondria by preventing Ca^{2+} efflux from organelles, also stops cell autonomic Ca^{2+} spiking. Our findings obtained using three Ca^{2+} or potential-sensitive probes in both quiescent and spontaneously spiking cells strongly suggest that IP_3 is able to create microdomains of high Ca^{2+} concentration around neighboring mitochondria. This event triggers a Ca^{2+} load and a depolarization of the organelles because Ca^{2+} around the mitochondrial uniporter reached the concentration required to open it (Rizzuto *et al.*, 1993, 1998). Ca^{2+} microdomains are more directly revealed in cardiac cells by the experiments using caffeine in Rhod2-loaded cells or in myocytes transfected with a mitochondria-targeted cameleon (Figure 7, C and D). Indeed, in contrast to focal release from the SR (Duchen *et al.*, 1998), a global cytosolic Ca^{2+} increase after caffeine addition to the cells in normal Na^+- and Ca^{2+}-containing extracellular buffer was not sensed by mitochondria. However, the organelles took up Ca^{2+} locally released by ATP or IP_3 from the caffeine-insensitive ER. This is in line with previous observations in cardiac cells in which caffeine induced a mitochondrial Ca^{2+} load only in Na^+- and Ca^{2+}-free medium, a condition that prevents activity of the Na^+/Ca^{2+} exchanger, the main Ca^{2+}-extruding mechanism in these cells (Bassani *et al.*, 1993). Ca^{2+} concentration can reach 100 μM close to the IP_3Rs (20-nm distance), a value 10-fold higher than the K_m of the mitochondrial Ca^{2+} uniporter, and can go down to 5–10 μM at a 200-nm distance as calculated for a voltage-gated channel (Neher, 1998). Thus, our findings suggest that mitochondria do not face the SR Ca^{2+}-releasing sites and that Ca^{2+} microdomains are not generated around them. In contrast, ER Ca^{2+}-releasing sites (i.e., IP_3Rs) are more likely to be in close connection with mitochondria (Figure 5B) in cardiomyocytes like in any other cell types because we also observed that IP_3 but not thapsigargin triggered a significant mitochondrial Ca^{2+} loading. In agreement with our observations in cardiomyocytes, thapsigargin or 2,5-di-(t-butyl)-1,4-hydroquinone (tBuBHQ) did not affect mitochondrial Ca^{2+} in RBL-2H3 (Csordas *et al.*, 1999) or in the MH75 cell line (Rizzuto *et al.*, 1994). However, BHQ and thapsigargin induced a Ca^{2+} uptake by mitochondria in chromaffin cells (Babcock *et al.*, 1997) and in hepatocytes, respectively (Hajnoczky *et al.*, 1995). This apparent discrepancy may be related to a different structure and/or spatial localization of the ER depending on the cell geometry. Together with the spatial distribution of IP_3Rs, primarily clustered, like mitochondria, around the nucleus, mitochondrial Ca^{2+} uptake is likely to account for the limited diffusion of Ca^{2+} locally released by IP_3 (Figure 1) and for the inability of

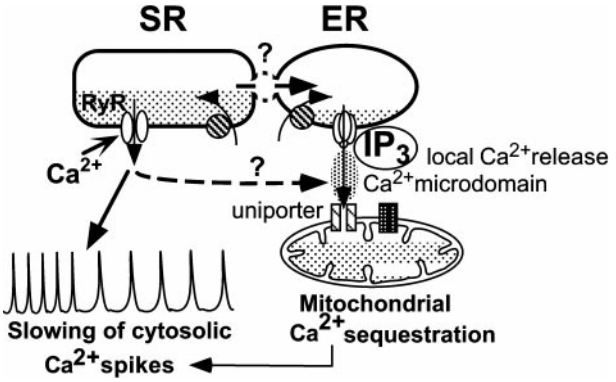

Figure 9. Diagram of the mechanism of IP_3-induced modulation of cytosolic Ca^{2+} oscillations: an integrated control of the filling state of the ER/SR and mitochondria. IP_3-induced Ca^{2+} release from the ER generates a high Ca^{2+} concentration in the vicinity of mitochondria. Thereby, mitochondria take up Ca^{2+} released by the IP_3-sensitive ER and trap part of the Ca^{2+}cycling from and into the SR through the uniporter. Alternatively, the SR may be in privileged communication with and may provide the ER with Ca^{2+} to refill after mitochondrial Ca^{2+} sequestration. In both situations, the SR is partially Ca^{2+}depleted, and in turn, cytosolic Ca^{2+} oscillations are slowed or stopped.

IP_3 to trigger CICR from the SR. This further supports the diffusion-limiting role of mitochondria in IP_3-dependent Ca^{2+} signals as observed in pancreatic cells (Tinel *et al.*, 1999). Ca^{2+} is then released from the organelles after depolarization of mitochondria (Sparagna *et al.*, 1995; Massari, 1996; Ichas *et al.*, 1997; Ichas and Mazat, 1998; Huser *et al.*, 1998) (Figure 7). Depending on the Ca^{2+}-loading state of mitochondria, their Ca^{2+} content can go below its initial value after IP_3-triggered Ca^{2+} uptake (Figure 7A) (Ichas *et al.*, 1997). This release prevents mitochondrial Ca^{2+} overload and refills the SR to regenerate Ca^{2+} transients.

We thus propose that part of the Ca^{2+} released from the SR with each beat flows into mitochondria through the Ca^{2+} uniporter (Bassani *et al.*, 1993; Duchen *et al.*, 1998; Ohata *et al.*, 1998; Zhou *et al.*, 1998) as the later is switched on by Ca^{2+} microdomains generated by IP_3. Alternatively, mitochondria may sequester only Ca^{2+} released by IP_3 from the ER, and Ca^{2+} could flow from the SR into the ER through a privileged communication between both stores (Figure 9). This would explain why the IP_3-induced Ca^{2+} release is faster in Ca^{2+} spiking (Figure 2) than in quiescent cells (Figure 1). Under these circumstances, the SR would also be transiently Ca^{2+} depleted, resulting in a slowing or arrest in cell Ca^{2+} spiking. To discriminate between these mechanisms further, we emptied mitochondrial Ca^{2+} or prevented efflux by using mitochondrial uncouplers (FCCP together with oligomycin) or a blocker of the permeability transition pore (cyclosporin A), respectively. These drugs however induced a large cytosolic Ca^{2+} transient that irreversibly blocks Ca^{2+} spiking (FCCP) or, like IP_3, slows (cyclosporin A; Figure 6A) spontaneous Ca^{2+} spiking of cardiomyocytes. Despite the fact that this prevented us from further testing the effect of IP_3 or ATP on these cells, the latter observation further supports the hypothesis that mitochondrial Ca^{2+}sequestration, whatever its origin, leads to a slowing of cytosolic Ca^{2+}spiking. Thus, these findings also provide evidence of a major role of mitochondria in closely regulating SR Ca^{2+} cycling. Because the firing of an action potential was slowed by ATP, it further suggests that Ca^{2+}-induced Ca^{2+} release closely modulates the generation of action potentials in these cardiomyocytes and in turn cellular automaticity, as it has been reported in pacemaker cells of the sinoatrial node (Ju and Allen, 1999).

Conclusions

We report that IP_3 and mitochondria are key components in the neurohumoral regulation of autonomic activity of neonatal rat cardiac cells, a reliable model of cellular automaticity. We bring a novel function of IP_3, as a modulator of cardiac rhythmic and autonomic activity. Although several IP_3-generating neurohormones including α_1-adrenergic, muscarinic, and purinergic agonists (Rosen *et al.*, 1988, 1990; Takikawa *et al.*, 1990; Terzic *et al.*, 1993) regulate cardiac rhythm, no direct proof of a critical role of IP_3 in gating cardiac rhythmic activity has been provided to date. The present findings show that in a beating cardiomyocyte, rhythmic Ca^{2+} oscillations are transiently blocked or slowed down while action potential firings are slowed down by an IP_3-induced spatially restricted Ca^{2+} release. Such a property of IP_3 may prove essential in preventing deleterious rhythmic accelerations (Hauswirth *et al.*, 1968), which could disrupt synchronous activity of the myocardium and provides a mechanistic basis for the previously established antiarrhythmic property of ATP. Thus, in addition to the CICR that is essential for cardiac excitation–contraction coupling, IP_3-triggered Ca^{2+} release may provide a previously unrecognized component in the regulation of cardiac rhythm of particular significance under physiological and pathological conditions associated with upregulated IP_3Rs (Marks, 1997). Furthermore, our findings implicate both an IP_3-sensitive Ca^{2+} store and mitochondria in regulating a major cell function. Such a coordinated mechanism may apply to other cell functions in excitable or nonexcitable tissues. These include the modulation of intracellular Ca^{2+} waves, as reported recently in astrocytes (Boitier *et al.*, 1999), the regulation of gene expression by Ca^{2+} spike frequency (Li *et al.*, 1998), and the excitability of neurons that also feature distinct ER and SR.

ACKNOWLEDGMENTS

We thank Dr. S. Roche (Centre de Recherches de Biochimie Macromoléculaire, Montpellier, France) for the generous gift of the anti-PLCγ antibody and the GST–SH2 fusion proteins, Drs. J. P. Mauger and M. Hilly (Institut National de la Santé et de la Recherche Médicale [INSERM], Orsay, France) for the kind gift of the anti-IP_3 receptor type I antibodies and for their continuous advice, Dr. J. B. Parys (Leuven University, Leuven, Belgium) for the kind gift of the anti-IP_3R type II antiserum, Dr. C. Erneux (Leuven University) for generously providing IP_3-5-phosphatase, Dr. Karl-Heinz Krause (University Medical Center, Geneva, Switzerland) for the gift of the anti-calreticulin antibody, R. Bortolon for his skillful assistance in confocal microscopy and image analysis at the LADM laboratory of the Mayo Foundation (Rochester, MN), and J. Terara for his skillful assistance in using the LSM-510 microscope at the Cell Imaging Facility of the Mayo Foundation. We thank Dr. N. Demaurex (University Medical Center) for the gift of cameleon, for the availability of the imaging setup in his laboratory to perform the experiments using cameleon, and for fruitful discussions. We also thank the

CRIC (Cell Imaging Resource, Montpellier, France) for assistance with the confocal micrographs of immunostained cells. M.J. was supported by INSERM. S.M.R. was supported by The Fondation Simon Del Duca (Paris, France).

REFERENCES

Adams, J.W., Sah, V.P., Henderson, S.A., and Brown, J.H. (1998). Tyrosine kinase and c-Jun NH2-terminal kinase mediate hypertrophic responses to prostaglandin F2α in cultured neonatal rat ventricular myocytes. Circ. Res. *83*, 167–178.

Antic, S., and Zecevic, D. (1995). Optical signals from neurons with internally applied voltage-sensitive dyes. J. Neurosci. *15*, 1392–1405.

Babcock, D.F., Herrington, J., Goodwin, P.C., Park, Y.B., and Hille, B. (1997). Mitochondrial participation in the intracellular Ca^{2+} network. J. Cell Biol. *136*, 833–844.

Bassani, J.W., Bassani, R.A., and Bers, D.M. (1993). Ca^{2+} cycling between sarcoplasmic reticulum and mitochondria in rabbit cardiac myocytes. J. Physiol. *460*, 603–621.

Berridge, M.J. (1993). Inositol trisphosphate and calcium signaling. Nature *361*, 315–325.

Boitier, E., Rea, R., and Duchen, M.R. (1999). Mitochondria exert a negative feedback on the propagation of intracellular Ca2+ waves in rat cortical astrocytes. J. Cell Biol. *145*, 795–808.

Brown, J.H., Buxton, I.L., and Brunton, L.L. (1985). Alpha 1-adrenergic and muscarinic cholinergic stimulation of phosphoinositide hydrolysis in adult rat cardiomyocytes. Circ. Res. *57*, 532–537.

Carroll, D.J., Ramarao, C.S., Mehlmann, L.M., Roche, S., Terasaki, M., and Jaffe, L.A. (1997). Calcium release at fertilization in starfish eggs is mediated by phospholipase Cgamma. J. Cell Biol. *138*, 1303–1311.

Chacon, E., Ohata, H., Harper, I.S., Trollinger, D.R., Herman, B., and Lemasters, J.J. (1996). Mitochondrial free calcium transients during excitation-contraction coupling in rabbit cardiac myocytes. FEBS Lett. *382*, 31–36.

Clapham, D.E. (1995). Calcium signaling. Cell *80*, 259–268.

Csordas, G., Thomas, A.P., and Hajnoczky, G. (1999). Quasi-synaptic calcium signal transmission between endoplasmic reticulum and mitochondria. EMBO J. *18*, 96–108.

Duchen, M.R., Leyssens, A., and Crompton, M. (1998). Transient mitochondrial depolarizations reflect focal sarcoplasmic reticular calcium release in single rat cardiomyocytes. J. Cell Biol. *142*, 975–988.

Fares, N., Bois, P., Lenfant, J., and Potreau, D. (1998). Characterization of a hyperpolarization-activated current in dedifferentiated adult rat ventricular cells in primary culture. J. Physiol. *506*, 73–82.

Felzen, B., Berke, G., Gardner, P., and Binah, O. (1997). Involvement of the IP3 cascade in the damage to guinea-pig ventricular myocytes induced by cytotoxic T lymphocytes. Pflügers Arch. *433*, 721–726.

Finch, E.A., and Augustine, G.J. (1998). Local calcium signaling by inositol-1,4,5-trisphosphate in Purkinje cell dendrites. Nature *396*, 753–756.

Fitzgerald, M., Neylon, C.B., Marks, A.R., and Woodcock, E.A. (1994). Reduced ryanodine receptor content in isolated neonatal cardiomyocytes compared with the intact tissue. J. Mol. Cell. Cardiol. *26*, 1261–1265.

Golovina, V.A., and Blaustein, M.P. (1997). Spatially and functionally distinct Ca^{2+} stores in sarcoplasmic and endoplasmic reticulum. Science *275*, 1643–1648.

Gomez, J.P., Potreau, D., Branka, J.E., and Raymond, G. (1994). Developmental changes in Ca^{2+} currents from newborn rat cardiomyocytes in primary culture. Pflügers Arch. *428*, 241–249.

Gorza, L., Schiaffino, S., and Volpe, P. (1993). Inositol 1,4,5-trisphosphate receptor in heart: evidence for its concentration in Purkinje myocytes of the conduction system. J. Cell Biol. *121*, 345–353.

Goutsouliak, V., and Rabkin, S.W. (1997). Angiotensin II-induced inositol phosphate generation is mediated through tyrosine kinase pathways in cardiomyocytes. Cell. Signal. *9*, 505–512.

Gunter, T.E., Gunter, K.K., Sheu, S.S., and Gavin, C.E. (1994). Mitochondrial calcium transport: physiological and pathological relevance. Am. J. Physiol. *267*, C313—C339.

Hajnoczky, G., Hager, R., and Thomas, A.P. (1999). Mitochondria suppress local feedback activation of inositol 1,4,5-trisphosphate receptors by Ca^{2+}. J. Biol. Chem. *274*, 14157–14162.

Hajnoczky, G., Robb-Gaspers, L.D., Seitz, M.B., and Thomas, A.P. (1995). Decoding of cytosolic calcium oscillations in the mitochondria. Cell *82*, 415–424.

Hauswirth, O., Noble, D., and Tsien, R.W. (1968). Adrenaline: mechanism of action on the pacemaker potential in cardiac Purkinje fibers. Science *162*, 916–917.

Hilal-Dandan, R., Urasawa, K., and Brunton, L.L. (1992). Endothelin inhibits adenylate cyclase and stimulates phosphoinositide hydrolysis in adult cardiac myocytes. J. Biol. Chem. *267*, 10620–10624.

Huser, J., Rechenmacher, C.E., and Blatter, L.A. (1998). Imaging the permeability pore transition in single mitochondria. Biophys. J. *74*, 2129–2137.

Ichas, F., Jouaville, L.S., and Mazat, J.P. (1997). Mitochondria are excitable organelles capable of generating and conveying electrical and calcium signals. Cell *89*, 1145–1153.

Ichas, F., and Mazat, J.P. (1998). From calcium signaling to cell death: two conformations for the mitochondrial permeability transition pore. Switching from low- to high-conductance state. Biochim. Biophys. Acta *1366*, 33–50.

Jacobsen, A.N., Du, X.J., Lambert, K.A., Dart, A.M., and Woodcock, E.A. (1996). Arrhythmogenic action of thrombin during myocardial reperfusion via release of inositol 1,4,5-triphosphate. Circulation *93*, 23–26.

Jaconi, M., Pyle, J., Bortolon, R., Ou, J., and Clapham, D. (1997). Calcium release and influx colocalize to the endoplasmic reticulum. Curr. Biol. *7*, 599–602.

Jongsma, H.J., Tsjernina, L., and de Bruijne, J. (1983). The establishment of regular beating in populations of pacemaker heart cells. A study with tissue-cultured rat heart cells. J. Mol. Cell. Cardiol. *15*, 123–133.

Ju, Y.K., and Allen, D.G. (1999). How does beta-adrenergic stimulation increase the heart rate? The role of intracellular Ca^{2+} release in amphibian pacemaker cells. J. Physiol. *516*, 793–804.

Kroner, H. (1992). The different routes of calcium efflux from liver mitochondria. Biol. Chem. Hoppe Seyler *373*, 229–235.

Li, W., Llopis, J., Whitney, M., Zlokarnik, G., and Tsien, R.Y. (1998). Cell-permeant caged InsP3 ester shows that Ca2+ spike frequency can optimize gene expression. Nature *392*, 936–941.

Lin, P., Yao, Y., Hofmeister, R., Tsien, R.Y., and Farquhar, M.G. (1999). Overexpression of CALNUC (Nucleobindin) increases agonist and thapsigargin releasable Ca^{2+} storage in the Golgi. J. Cell Biol. *145*, 279–289.

Loew, L.M., Carrington, W., Tuft, R.A., and Fay, F.S. (1994). Physiological cytosolic Ca^{2+} transients evoke concurrent mitochondrial depolarizations. Proc. Natl. Acad. Sci. USA *91*, 12579–12583.

Maltsev, V.A., Wobus, A.M., Rohwedel, J., Bader, M., and Hescheler, J. (1994). Cardiomyocytes differentiated in vitro from embryonic stem cells developmentally express cardiac-specific genes and ionic currents. Circ. Res. *75*, 233–244.

Marks, A.R. (1997). Intracellular calcium-release channels: regulators of cell life and death. Am. J. Physiol. *272*, H597–H605.

Massari, S. (1996). Kinetic analysis of the mitochondrial permeability transition. J. Biol. Chem. *271*, 31942–31948.

Mikoshiba, K., Furuichi, T., and Miyawaki, A. (1994). Structure and function of IP_3 receptors. Semin. Cell Biol. *5*, 273–281.

Miyawaki, A., Llopis, J., Heim, R., McCaffery, J.M., Adams, J.A., Ikura, M., and Tsien, R.Y. (1997). Fluorescent indicators for Ca^{2+} based on green fluorescent proteins and calmodulin. Nature *388*, 882–887.

Moses, R.L., and Kasten, F.H. (1979). T-tubes in cultured mammalian myocardial cells. Cell Tissue Res. *203*, 173–180.

Murthy, K.S., and Makhlouf, G.M. (1998). Coexpression of ligand-gated P-2X and G protein-coupled P-2Y receptors in smooth muscle. Preferential activation of P-2Y receptors coupled to phospholipase C (PLC)-β1 via G$\forall$q/1 and the PLC-β3 via G $\beta\gamma$(i3). J. Biol. Chem. *273*, 4695–4704.

Neher, E. (1998). Vesicle pools and Ca^{2+} microdomains: new tools for understanding their roles in neurotransmitter release. Neuron *20*, 389–399.

Ohata, H., Chacon, E., Tesfai, S.A., Harper, I.S., Herman, B., and Lemasters, J.J. (1998). Mitochondrial Ca^{2+} transients in cardiac myocytes during the excitation-contraction cycle: effects of pacing and hormonal stimulation. J. Bioenerg. Biomembr. *30*, 207–222.

Parys, J.B., de Smedt, H., Missiaen, L., Bootman, M.D., Sienaert, I., and Casteels, R. (1995). Rat basophilic leukemia cells as model system for inositol 1,4,5-trisphosphate receptor IV, a receptor of the type II family: functional comparison and immunological detection. Cell Calcium *17*, 239–249.

Pinton, P., Pozzan, T., and Rizzuto, R. (1998). The Golgi apparatus is an inositol 1,4,5-trisphosphate-sensitive Ca2+ store, with functional properties distinct from those of the endoplasmic reticulum. EMBO J. *17*, 5298–5308.

Puceat, M., Clement, O., Scamps, F., and Vassort, G. (1991). Extracellular ATP-induced acidification leads to cytosolic calcium transient rise in single rat cardiac myocytes. Biochem. J. *274*, 55–62.

Puceat, M., Hilal-Dandan, R., Strulovici, B., Brunton, L.L., and Brown, J.H. (1994). Differential regulation of protein kinase C isoforms in isolated neonatal and adult rat cardiomyocytes. J. Biol. Chem. *269*, 16938–16944.

Puceat, M., Korichneva, I., Cassoly, R., and Vassort, G. (1995). Identification of band 3-like proteins and Cl^-/HCO_3^- exchange in isolated cardiomyocytes. J. Biol. Chem. *270*, 1315–1322.

Puceat, M., Roche, S., and Vassort, G. (1998). Src family tyrosine kinase regulates intracellular pH in cardiomyocytes. J. Cell Biol. *141*, 1637–1646.

Puceat, M., and Vassort, G. (1996). Purinergic stimulation of rat cardiomyocytes induces tyrosine phosphorylation and membrane association of phospholipase Cγ: a major mechanism for $InsP_3$ generation. Biochem. J. *318*, 723–728.

Rizzuto, R., Bastianutto, C., Brini, M., Murgia, M., and Pozzan, T. (1994). Mitochondrial Ca^{2+} homeostasis in intact cells. J. Cell Biol. *126*, 1183–1194.

Rizzuto, R., Brini, M., Murgia, M., and Pozzan, T. (1993). Microdomains with high Ca^{2+} close to IP_3-sensitive channels that are sensed by neighboring mitochondria. Science *262*, 744–747.

Rizzuto, R., Pinton, P., Carrington, W., Fay, F.S., Fogarty, K.E., Lifshitz, L.M., Tuft, R.A., and Pozzan, T. (1998). Close contacts with the endoplasmic reticulum as determinants of mitochondrial Ca^{2+} responses. Science *280*, 1763–1766.

Robert, V., De Giorgi, F., Massimino, M.L., Cantini, M., and Pozzan, T. (1998). Direct monitoring of the calcium concentration in the sarcoplasmic and endoplasmic reticulum of skeletal muscle myotubes. J. Biol. Chem. *273*, 30372–30378.

Roche, S., McGlade, J., Jones, M., Gish, G.D., Pawson, T., and Courtneidge, S.A. (1996). Requirement of phospholipase C gamma, the tyrosine phosphatase Syp and the adaptor proteins Shc and Nck for PDGF-induced DNA synthesis: evidence for the existence of Ras-dependent and Ras-independent pathways. EMBO J. *15*, 4940–4948.

Roderick, H.L., Campbell, A.K., and Llewellyn, D.H. (1997). Nuclear localisation of calreticulin in vivo is enhanced by its interaction with glucocorticoid receptors. FEBS Lett. *405*, 181–185.

Rosen, M.R., Danilo, P., Jr., Robinson, R.B., Shah, A., and Steinberg, S.F. (1988). Sympathetic neural and alpha-adrenergic modulation of arrhythmias. Ann. NY Acad. Sci. *533*, 200–209.

Rosen, M.R., Steinberg, S.F., and Danilo, P., Jr. (1990). Developmental changes in the muscarinic stimulation of canine Purkinje fibers. J. Pharmacol. Exp. Ther. *254*, 356–361.

Saeki, T., Shen, J.-B., and Pappano, A.J. (1999). Inositol-1,4,5-trisphosphate increases contractions but not L-type calcium current in guinea pig ventricular myocytes. Cardiovasc. Res. *41*, 620–628.

Scamps, F., and Carmeliet, E. (1989). Effect of external K+ on the delayed K+ current in single rabbit Purkinje cells. Pflügers Arch. *414*(suppl 1), S169—S170.

Sparagna, G.C., Gunter, K.K., Sheu, S.S., and Gunter, T.E. (1995). Mitochondrial calcium uptake from physiological-type pulses of calcium. A description of the rapid uptake mode. J. Biol. Chem. *270*, 27510–27515.

Takikawa, R., Kurachi, Y., Mashima, S., and Sugimoto, T. (1990). Adenosine-5′-triphosphate-induced sinus tachycardia mediated by prostaglandin synthesis via phospholipase C in the rabbit heart. Pflügers Arch. *417*, 13–20.

Terzic, A., Puceat, M., Vassort, G., and Vogel, S.M. (1993). Cardiac alpha 1-adrenoceptors: an overview. Pharmacol. Rev. *45*, 147–175.

Tinel, H., Cancela, J.M., Mogami, H., Gerasimenko, J.V., Gerasimenko, O.V., Tepikin, A.V., and Petersen, O.H. (1999). Active mitochondria surrounding the pancreatic acinar granule region prevent spreading of inositol trisphosphate-evoked local cytosolic Ca^{2+} signals. EMBO J. *18*, 4999–5008.

Vassort, G., Puceat, M., and Scamps, F. (1994). Modulation of myocardial activity by extracellular ATP. Trends Cardiovasc. Med. *4*, 236–240.

Zhou, Z., Matlib, M.A., and Bers, D.M. (1998). Cytosolic and mitochondrial Ca^{2+} signals in patch clamped mammalian ventricular myocytes. J. Physiol. *507*, 379–403.